

Electroweak form factors of non-strange baryons

D. Merten^a, U. Löring, K. Kretzschmar, B. Metsch, and H.-R. Petry

Institut für Theoretische Kernphysik, Nußallee 14–16, D-53115 Bonn, Germany

Received: 4 April 2002

Communicated by V.V. Anisovich

Abstract. We compute electroweak form factors of the nucleon and photon transition form factors of non-strange baryon resonances up to the third resonance region in a model with instanton-induced interaction. The calculation is based on the Bethe-Salpeter equation for three light constituent quarks and is fully relativistic (U. Löring *et al.*, Eur. Phys. J. A **10**, 309 (2001)). Static nucleon properties and photon resonance couplings are in good agreement with experiment and the Q^2 behaviour of the experimentally known form factors up to large momentum transfer is accounted for.

PACS. 11.10.St Bound and unstable states; Bethe-Salpeter equations – 12.39.Ki Relativistic quark model – 13.40.Gp Electromagnetic form factors

1 Introduction

The notion of constituent quarks has proven to be the most successful concept for the interpretation of hadron resonances. We know, however, that they can, at best, be quasi-particles which arise due to a dynamical breakdown of chiral symmetry in fundamental QCD. The details of this process are still obscure; we believe, therefore, that it is of general interest to work out precisely at which energies this concept tends to fail. As a first step it is therefore necessary to construct a constituent quark model, which fits the mass spectrum quantitatively, and to extend this model in energy and momentum transfer as much as possible. For this reason the following issues are the most essential for our approach:

1. The model has to be relativistic covariant. This is obviously not the case in non-relativistic quark models, which dominated the research of the last decades [1]. The need for covariance was clearly recognised in the past, and led to various relativizations (*e.g.* [2,3]). They include in particular the use of formally relativistic energies and a prescription for boosting non-relativistic wave functions. The importance of this last point was recently demonstrated again by the Graz group [4]. In contrast to this, we have directly used in our attempts the Bethe-Salpeter equation with instantaneous forces, which respects covariance right from the beginning. This model was used for light quark flavours with considerable success concerning the spectrum of mesons [5] and baryons [6–8]. With only 7 model parameters (masses and couplings) an efficient

and good description of the experimentally known baryon spectrum could be achieved describing both Regge trajectories and the fine structure in the mass splittings.

2. Usual non-relativistic quark interactions (string-like confinement and one-gluon exchange fine-structure interaction) have proven to lead to inconsistent spectroscopic results, *e.g.* too large spin-orbit couplings. In addition, the known nucleon Regge trajectory is not correctly explained. In our model we keep the string-like confinement and solve the spin-orbit problem by an appropriate Dirac structure. We also replace the one-gluon exchange by 't Hooft's instanton-induced interaction [9,10]. This has the advantage that the $U_A(1)$ anomaly of the meson spectrum is correctly treated and that the η' problem is convincingly solved from the very beginning. In addition, the 't Hooft's force is very similar in structure to the dynamics of a Nambu-Jona-Lasinio model and offers a natural mechanism for chiral symmetry breaking (see [11,12]).

The model we have constructed, however, not only describes the hadron mass spectrum; the basic Bethe-Salpeter amplitudes we computed can be used to derive form factors and couplings of various sorts [13]. Such a calculation has already been published for mesonic states alone [5]. In this paper we show now a more or less complete calculation of electroweak nucleon form factors and resonance transition form factors as far as experimental data are available. We limit ourselves to non-strange baryons; baryons with strangeness will be considered in another publication.

The present paper is organized as follows:

^a e-mail: merten@itkp.uni-bonn.de

- a) In the first section we outline the theoretical derivation of our form factors. For more details of the model itself we refer to our previous publications [6–8]. Here we only describe the way how current matrix elements follow from the Bethe-Salpeter equation. Particular emphasis is put on the treatment of the quark two-body interaction and its role in the three-body vertex function (see also appendix A).
- b) In sect. 2 we show our results for the nucleonic electroweak form factors in comparison to the experiment. Several theoretical aspects are discussed in addition, in particular, the special effects of the quark interaction and the relevance of relativistic boosting.
- c) In sect. 3 we present our predictions for transition form factors. We compare with various experimental data, which are, however, not as well established as it is the case for the nucleon properties, because the extraction of these form factors from pion photoproduction is highly model dependent. Less ambiguous are the photon couplings (helicity amplitudes), for which we have indeed results, which show good overall agreement with the known data. The detailed behaviour of these form factors as a function of Q^2 shows, however, sometimes large discrepancies with the functional behaviour extracted so far from experiments. Our results can in this respect be regarded as alternative predictions waiting for experimental verification.

At the end of this introduction we want to stress that the calculation presented in this paper contains no free parameters or normalization. All model parameters were fixed in the previous calculation of the baryon mass spectrum [7]. (We use the set of model \mathcal{A} from this reference which quantitatively describes several features of the complete light flavour baryon spectrum.) We even did not try to bring our form factor results into closer agreement to some experimental values, when the disagreement was only due to slight deviations of our model resonance masses from the known experimental values, in order to be entirely consistent with our final goal to see how far the constituent quark picture of hadron resonances works in phenomenology at higher energies.

2 Current matrix elements derived from the Bethe-Salpeter amplitudes

2.1 Bethe-Salpeter amplitudes

In our first paper [6] we presented a formally covariant constituent quark model of baryons which is based on the 3-quark Bethe-Salpeter amplitudes

$$\chi_{\bar{P} a_1 a_2 a_3}(x_1, x_2, x_3) := \langle 0 | T \Psi_{a_1}(x_1) \Psi_{a_2}(x_2) \Psi_{a_3}(x_3) | \bar{P} \rangle. \quad (1)$$

In quantum field theory these are the transition matrix elements of three-quark field operators $\Psi_{a_i}(x_i)$ between a baryon state $|\bar{P}\rangle$ with mass $M = \sqrt{\bar{P}^2}$ and four-momentum $\bar{P} = (\omega_{\mathbf{P}}, \mathbf{P}) = (\sqrt{|\mathbf{P}|^2 + M^2}, \mathbf{P})$ and the vacuum $|0\rangle$. The Fourier transform $\chi_{\bar{P}}(p_\xi, p_\eta)$ (here p_ξ and

and p_η are the two relative Jacobi four-momenta) formally obeys the Bethe-Salpeter equation which in a shorthand operator notation reads

$$\chi_{\bar{P}} = -i G_{0\bar{P}} \left(K_{\bar{P}}^{(3)} + \overline{K}_{\bar{P}}^{(2)} \right) \chi_{\bar{P}}. \quad (2)$$

Here $G_{0\bar{P}}$ denotes the three-fold tensor product

$$\begin{aligned} G_{0\bar{P}}(p_\xi, p_\eta; p'_\xi, p'_\eta) = & S_F^1\left(\frac{1}{3}P + p_\xi + \frac{1}{2}p_\eta\right) \otimes S_F^2\left(\frac{1}{3}P - p_\xi + \frac{1}{2}p_\eta\right) \otimes S_F^3\left(\frac{1}{3}P - p_\eta\right) \\ & \times (2\pi)^4 \delta^{(4)}(p_\xi - p'_\xi) (2\pi)^4 \delta^{(4)}(p_\eta - p'_\eta) \end{aligned} \quad (3)$$

of full quark propagators S_F^i , $K_{\bar{P}}^{(3)}$ is the irreducible three-body interaction kernel and $\overline{K}_{\bar{P}}^{(2)}$ the sum

$$\begin{aligned} \overline{K}_{\bar{P}}^{(2)}(p_\xi, p_\eta; p'_\xi, p'_\eta) = & K_{\left(\frac{2}{3}P + p_\eta\right)}^{(2)}(p_\xi, p'_\xi) \otimes S_F^3{}^{-1}\left(\frac{1}{3}P - p_\eta\right) (2\pi)^4 \delta^{(4)}(p_\eta - p'_\eta) \\ & + \text{corresponding terms with interacting} \\ & \text{quark pairs (23) and (31)} \end{aligned} \quad (4)$$

of the irreducible two-particle interactions $K^{(2)}$ in each quark pair.

To be as close as possible in contact with the quite successful non-relativistic quark model, the basic assumptions of this model are the following:

1. The full quark propagators S_F^i are replaced by free Feynman propagators with effective constituent quark masses m_i :

$$S_F^i(p_i) \stackrel{!}{=} \frac{i}{\not{p}_i - m_i + i\epsilon}. \quad (5)$$

2. We adopt instantaneous three- and two-body interaction kernels $K^{(3)}$ and $K^{(2)}$ which in the rest frame of the baryon are described by the unretarded three- and two-body potentials $V^{(3)}$ and $V^{(2)}$:

$$K_{\bar{P}}^{(3)}(p_\xi, p_\eta; p'_\xi, p'_\eta) \Big|_{P=(M,0)} \stackrel{!}{=} V^{(3)}(\mathbf{p}_\xi, \mathbf{p}_\eta; \mathbf{p}'_\xi, \mathbf{p}'_\eta), \quad (6)$$

$$K_{\left(\frac{2}{3}P + p_\eta\right)}^{(2)}(p_\xi, p'_\xi) \Big|_{P=(M,0)} \stackrel{!}{=} V^{(2)}(\mathbf{p}_\xi, \mathbf{p}'_\xi).$$

In our specific quark model of baryons [7,8] these potentials represent the string-like confinement for the three-particle kernel and the 't Hooft's instanton-induced interaction for the two-particle kernel.

These assumptions allow to eliminate the energy-like coordinates p_ξ^0 and p_η^0 and thus to reduce the 3-fermion Bethe-Salpeter equation to a simpler equation —known as Salpeter equation. In case of instantaneous three-body forces alone this reduction procedure is straightforward. However, as discussed in detail in ref. [6], serious complications arise within the reduction procedure, if genuine 2-body interactions are taken into account in the three-body Bethe-Salpeter equation: the unconnected two-body

contribution $\overline{K}_P^{(2)}$ within the three-body system then prevents a straightforward reduction to the Salpeter equation. In ref. [6] we presented a method which—in presence of a genuine instantaneous three-body kernel—nevertheless allows a reasonable treatment of these forces within the Salpeter framework. There, we derived a Salpeter equation for the (projected) Salpeter amplitude (for a brief review see also appendix A)

$$\begin{aligned} \Phi_M^A(\mathbf{p}_\xi, \mathbf{p}_\eta) &:= (\Lambda^{+++}(\mathbf{p}_\xi, \mathbf{p}_\eta) + \Lambda^{---}(\mathbf{p}_\xi, \mathbf{p}_\eta)) \\ &\times \int \frac{d^3 p_\xi^0}{2\pi} \frac{d^3 p_\eta^0}{2\pi} \chi_M((p_\xi^0, \mathbf{p}_\xi), (p_\eta^0, \mathbf{p}_\eta)), \end{aligned} \quad (7)$$

where $\Lambda^{+++}(\mathbf{p}_\xi, \mathbf{p}_\eta) := \Lambda_1^+(\mathbf{p}_1) \otimes \Lambda_2^+(\mathbf{p}_2) \otimes \Lambda_3^+(\mathbf{p}_3)$ and $\Lambda^{---}(\mathbf{p}_\xi, \mathbf{p}_\eta) := \Lambda_1^-(\mathbf{p}_1) \otimes \Lambda_2^-(\mathbf{p}_2) \otimes \Lambda_3^-(\mathbf{p}_3)$ are projection operators onto purely positive-energy and purely negative-energy three-quark states, respectively. This is achieved by a perturbative elimination of retardation effects which arise due to the two-body interaction. To this end we constructed an instantaneous three-body kernel V_M^{eff} which effectively parameterizes the effects of the two-body forces. We expanded this quasi-potential in powers of a residual kernel $K_M^R = \overline{K}_M^{(2)} + V_R^{(3)}$ which is the sum of the retarded two-body contribution $\overline{K}_M^{(2)}$ and that part $V_R^{(3)}$ of the instantaneous three-body kernel $V^{(3)}$ that couples to the mixed energy components. In the lowest order (Born approximation) $V_M^{\text{eff}} \approx V_M^{\text{eff}(1)}$ of this perturbative expansion one finds

$$\begin{aligned} V_M^{\text{eff}(1)}(\mathbf{p}_\xi, \mathbf{p}_\eta; \mathbf{p}'_\xi, \mathbf{p}'_\eta) &= \\ &(2\pi)^3 \delta^{(3)}(\mathbf{p}_\eta - \mathbf{p}'_\eta) \gamma^0 \otimes \gamma^0 \otimes \gamma^0 \\ &\times \left[\Lambda^{+++}(\mathbf{p}_\xi, \mathbf{p}_\eta) \left[\gamma^0 \otimes \gamma^0 V^{(2)}(\mathbf{p}_\xi, \mathbf{p}'_\xi) \right] \otimes \mathbf{1} \Lambda^{+++}(\mathbf{p}'_\xi, \mathbf{p}_\eta) \right. \\ &\left. - \Lambda^{---}(\mathbf{p}_\xi, \mathbf{p}_\eta) \left[\gamma^0 \otimes \gamma^0 V^{(2)}(\mathbf{p}_\xi, \mathbf{p}'_\xi) \right] \otimes \mathbf{1} \Lambda^{---}(\mathbf{p}'_\xi, \mathbf{p}_\eta) \right] \\ &+ \text{corresponding terms with interacting} \\ &\quad \text{quark pairs (23) and (31),} \end{aligned} \quad (8)$$

and the Salpeter equation then reads explicitly as follows:

$$\begin{aligned} \Phi_M^A(\mathbf{p}_\xi, \mathbf{p}_\eta) &= \\ &\times \left[\frac{\Lambda^{+++}(\mathbf{p}_\xi, \mathbf{p}_\eta)}{M - \Omega(\mathbf{p}_\xi, \mathbf{p}_\eta) + i\epsilon} + \frac{\Lambda^{---}(\mathbf{p}_\xi, \mathbf{p}_\eta)}{M + \Omega(\mathbf{p}_\xi, \mathbf{p}_\eta) - i\epsilon} \right] \gamma^0 \otimes \gamma^0 \otimes \gamma^0 \\ &\times \int \frac{d^3 p'_\xi}{(2\pi)^3} \frac{d^3 p'_\eta}{(2\pi)^3} V^{(3)}(\mathbf{p}_\xi, \mathbf{p}_\eta; \mathbf{p}'_\xi, \mathbf{p}'_\eta) \Phi_M^A(\mathbf{p}'_\xi, \mathbf{p}'_\eta) \\ &+ \left[\frac{\Lambda^{+++}(\mathbf{p}_\xi, \mathbf{p}_\eta)}{M - \Omega(\mathbf{p}_\xi, \mathbf{p}_\eta) + i\epsilon} - \frac{\Lambda^{---}(\mathbf{p}_\xi, \mathbf{p}_\eta)}{M + \Omega(\mathbf{p}_\xi, \mathbf{p}_\eta) - i\epsilon} \right] \gamma^0 \otimes \gamma^0 \otimes \mathbf{1} \\ &\times \int \frac{d^3 p'_\xi}{(2\pi)^3} V^{(2)}(\mathbf{p}_\xi, \mathbf{p}'_\xi) \otimes \mathbf{1} \Phi_M^A(\mathbf{p}'_\xi, \mathbf{p}_\eta) \\ &+ \text{corresponding terms with interacting} \\ &\quad \text{quark pairs (23) and (31).} \end{aligned} \quad (9)$$

Here $\Omega(\mathbf{p}_\xi, \mathbf{p}_\eta) := \omega_1(\mathbf{p}_1) + \omega_2(\mathbf{p}_2) + \omega_3(\mathbf{p}_3)$ denotes the sum of the kinetic energies $\omega_i(\mathbf{p}_i) = \sqrt{|\mathbf{p}_i|^2 + m_i^2}$ of each quark. This equation determines the baryon masses M and the corresponding Salpeter amplitudes Φ_M^A . The full Bethe-Salpeter amplitude $\chi_{\bar{P}}$ in the corresponding order of approximation is then determined from the Salpeter amplitude Φ_M^A as follows (for details see appendix A):

$$\chi_{\bar{P}} = \left[G_{0\bar{P}} - iG_{0\bar{P}} \left(V_R^{(3)} + \overline{K}_{\bar{P}}^{(2)} - V_{\bar{P}}^{\text{eff}(1)} \right) G_{0\bar{P}} \right] \Gamma_{\bar{P}}^A, \quad (10)$$

where we introduced the vertex function Γ_M^A according to

$$\begin{aligned} \Gamma_M^A(\mathbf{p}_\xi, \mathbf{p}_\eta) &:= -i \int \frac{d^3 p'_\xi}{(2\pi)^3} \frac{d^3 p'_\eta}{(2\pi)^3} \\ &\left[V_A^{(3)}(\mathbf{p}_\xi, \mathbf{p}_\eta; \mathbf{p}'_\xi, \mathbf{p}'_\eta) + V_M^{\text{eff}(1)}(\mathbf{p}_\xi, \mathbf{p}_\eta; \mathbf{p}'_\xi, \mathbf{p}'_\eta) \right] \Phi_M^A(\mathbf{p}'_\xi, \mathbf{p}'_\eta). \end{aligned} \quad (11)$$

Here the baryon four-momentum $\bar{P} = M = (M, \mathbf{0})$ is at rest; for a general four-momentum \bar{P} on the mass shell the vertex function must be boosted by a suitable Lorentz transformation in the obvious way.

2.2 Current matrix elements

The physically relevant bound-state matrix elements of the current operator $\langle \bar{P} | j^\mu(x) | \bar{P}' \rangle$ with

$$j^\mu(x) := : \bar{\Psi}(x) \hat{q} \gamma^\mu \Psi(x) :,$$

where \hat{q} is the charge operator, are calculated as follows: First consider the eight-point Green's function

$$\begin{aligned} G^\mu(x_1, x_2, x_3, x, x'_1, x'_2, x'_3) &= \\ &-\langle 0 | T \Psi(x_1) \Psi(x_2) \Psi(x_3) j^\mu(x) \bar{\Psi}(x'_1) \bar{\Psi}(x'_2) \bar{\Psi}(x'_3) | 0 \rangle. \end{aligned} \quad (12)$$

Fixing the specific time ordering

$$\min\{x_1^0, x_2^0, x_3^0\} > x^0 > \max\{x'_1{}^0, x'_2{}^0, x'_3{}^0\}$$

and inserting the physical baryon states $|\bar{P}\rangle$ and $|\bar{P}'\rangle$ in-between, we find that the Fourier transform of this quantity must have poles at $P^0 = \omega_{\mathbf{P}} := \sqrt{|\mathbf{P}|^2 + M^2}$ and $P'^0 = \omega'_{\mathbf{P}'} := \sqrt{|\mathbf{P}'|^2 + M'^2}$. In the vicinity of these poles the Fourier transform $G_{P, P'}^\mu$ of G^μ has the form

$$\begin{aligned} G_{P, P'}^\mu(p_\xi, p_\eta, p'_\xi, p'_\eta) &= \\ &\frac{1}{4 \omega_{\mathbf{P}} \omega'_{\mathbf{P}'}} \frac{\chi_{\bar{P}}(p_\xi, p_\eta)}{(P^0 - \omega_{\mathbf{P}} + i\epsilon)} \langle \bar{P} | j^\mu(0) | \bar{P}' \rangle \frac{\overline{\chi}_{\bar{P}'}(p'_\xi, p'_\eta)}{(P'^0 - \omega'_{\mathbf{P}'} + i\epsilon)} \\ &+ \text{regular terms for } P^0 \rightarrow \omega_{\mathbf{P}} \text{ and } P'^0 \rightarrow \omega'_{\mathbf{P}'}. \end{aligned} \quad (13)$$

On the other hand, the minimal coupling yields

$$\begin{aligned} G_{P, P'}^\mu(p_\xi, p_\eta, p'_\xi, p'_\eta) &= \\ &\int \frac{d^4 p''_\xi}{(2\pi)^4} \frac{d^4 p''_\eta}{(2\pi)^4} \frac{d^4 p'''_\xi}{(2\pi)^4} \frac{d^4 p'''_\eta}{(2\pi)^4} G_P(p_\xi, p_\eta; p''_\xi, p''_\eta) \\ &\times K_{P, P'}^\mu(p''_\xi, p''_\eta, p'''_\xi, p'''_\eta) \\ &\times G_{P'}(p'''_\xi, p'''_\eta; p'_\xi, p'_\eta). \end{aligned} \quad (14)$$

Here G_P is the Fourier transform of the six-point function

$$G(x_1, x_2, x_3; x'_1, x'_2, x'_3) := -\langle 0 | T \Psi(x_1) \Psi(x_2) \Psi(x_3) \bar{\Psi}(x'_1) \bar{\Psi}(x'_2) \bar{\Psi}(x'_3) | 0 \rangle. \quad (15)$$

$K_{P,P'}^\mu$ denotes the current kernel in momentum space which due to the presence of a 2-body interaction kernel is given by the sum

$$K_{P,P'}^\mu = K_{P,P'}^{\mu(0)} + K_{P,P'}^{\mu(1)} \quad (16)$$

with

$$\begin{aligned} K_{P,P'}^{\mu(0)}(p_\xi, p_\eta, p'_\xi, p'_\eta) = & S_F^{1-1} \left(\frac{1}{3}P + p_\xi + \frac{1}{2}p_\eta \right) \otimes S_F^{2-1} \left(\frac{1}{3}P - p_\xi + \frac{1}{2}p_\eta \right) \otimes \hat{q} \gamma^\mu \\ & \times (2\pi)^4 \delta^{(4)}(p_\xi - p'_\xi) (2\pi)^4 \delta^{(4)} \left(\frac{2}{3}(P - P') + p_\eta - p'_\eta \right) \\ & + \text{corresponding photon couplings to quarks 1 and 2} \end{aligned} \quad (17)$$

and

$$\begin{aligned} K_{P,P'}^{\mu(1)}(p_\xi, p_\eta, p'_\xi, p'_\eta) = & i K_{\left(\frac{2}{3}P + p_\eta\right)}^{\mu(2)}(p_\xi, p'_\xi) \otimes \hat{q} \gamma^\mu \\ & \times (2\pi)^4 \delta^{(4)} \left(\frac{2}{3}(P - P') + p_\eta - p'_\eta \right) \\ & + \text{corresponding terms with photon couplings} \\ & \text{to quark 1 and quark 2.} \end{aligned} \quad (18)$$

We now note (see ref. [6]) that the six-point Green's functions G_P and $G_{P'}$ in the vicinity of the baryon energies $P^0 = \omega_{\mathbf{P}}$ and $P'^0 = \omega'_{\mathbf{P}'}$, respectively, behave as

$$G_P(p_\xi, p_\eta; p'_\xi, p'_\eta) = \frac{-i}{2\omega_{\mathbf{P}}} \frac{\chi_{\bar{P}}(p_\xi, p_\eta) \bar{\chi}_{\bar{P}}(p'_\xi, p'_\eta)}{P^0 - \omega_{\mathbf{P}} + i\epsilon} + \text{regular terms for } P^0 \rightarrow \omega_{\mathbf{P}} \quad (19)$$

and

$$G_{P'}(p_\xi, p_\eta; p'_\xi, p'_\eta) = \frac{-i}{2\omega'_{\mathbf{P}'}} \frac{\chi_{\bar{P}'}(p_\xi, p_\eta) \bar{\chi}_{\bar{P}'}(p'_\xi, p'_\eta)}{P'^0 - \omega'_{\mathbf{P}'} + i\epsilon} + \text{regular terms for } P'^0 \rightarrow \omega'_{\mathbf{P}'} \quad (20)$$

Inserting these Laurent expansions of G_P and $G_{P'}$ into the previous equation (14) yields

$$\begin{aligned} G_{P,P'}^\mu(p_\xi, p_\eta, p'_\xi, p'_\eta) = & -\frac{1}{4\omega_{\mathbf{P}}\omega'_{\mathbf{P}'}} \frac{\chi_{\bar{P}}(p_\xi, p_\eta)}{(P^0 - \omega_{\mathbf{P}} + i\epsilon)} \\ & \times \left[\int \frac{d^4 p''_\xi}{(2\pi)^4} \frac{d^4 p''_\eta}{(2\pi)^4} \frac{d^4 p'''_\xi}{(2\pi)^4} \frac{d^4 p'''_\eta}{(2\pi)^4} \right. \\ & \left. \bar{\chi}_{\bar{P}}(p''_\xi, p''_\eta) K_{\bar{P},\bar{P}'}^\mu(p''_\xi, p''_\eta, p'''_\xi, p'''_\eta) \chi_{\bar{P}}(p'''_\xi, p'''_\eta) \right] \\ & \times \frac{\bar{\chi}_{\bar{P}}(p'_\xi, p'_\eta)}{(P'^0 - \omega'_{\mathbf{P}'} + i\epsilon)} \\ & + \text{regular terms for } P^0 \rightarrow \omega_{\mathbf{P}} \text{ and } P'^0 \rightarrow \omega'_{\mathbf{P}'}. \end{aligned} \quad (21)$$

The comparison with eq. (13) shows indeed that the formula

$$\begin{aligned} \langle \bar{P} | j^\mu(0) | \bar{P}' \rangle = & -\bar{\chi}_{\bar{P}} K_{\bar{P},\bar{P}'}^\mu \chi_{\bar{P}'} = \\ & - \int \frac{d^4 p_\xi}{(2\pi)^4} \frac{d^4 p_\eta}{(2\pi)^4} \frac{d^4 p'_\xi}{(2\pi)^4} \frac{d^4 p'_\eta}{(2\pi)^4} \\ & \bar{\chi}_{\bar{P}}(p_\xi, p_\eta) K_{\bar{P},\bar{P}'}^\mu(p_\xi, p_\eta, p'_\xi, p'_\eta) \chi_{\bar{P}'}(p'_\xi, p'_\eta) \end{aligned} \quad (22)$$

must hold. Our equations (10) and (16) for $\chi_{\bar{P}}$ and the current kernel $K_{\bar{P},\bar{P}'}$ can now be inserted into this formula. The result is

$$\langle \bar{P} | j^\mu(0) | \bar{P}' \rangle = -\bar{\chi}_{\bar{P}} K_{\bar{P},\bar{P}'}^\mu \chi_{\bar{P}'} = -\bar{\Gamma}_{\bar{P}}^A \mathcal{K}_{\bar{P},\bar{P}'}^\mu \Gamma_{\bar{P}'}^A, \quad (23)$$

where $\bar{\Gamma}_{\bar{P}}^A$ is the adjoint vertex function which in the rest frame of the baryon is related to $\Gamma_{\bar{P}}^A$ by

$$\bar{\Gamma}_M^A = -\Gamma_M^{A\dagger} \gamma^0 \otimes \gamma^0 \otimes \gamma^0. \quad (24)$$

$\mathcal{K}_{\bar{P},\bar{P}'}^\mu$ defines the effective current kernel

$$\begin{aligned} \mathcal{K}_{\bar{P},\bar{P}'}^\mu := & \left[G_{0\bar{P}} - i G_{0\bar{P}} \left(V_R^{(3)} + \bar{K}_{\bar{P}}^{(2)} - V_{\bar{P}}^{\text{eff}(1)} \right) G_{0\bar{P}} \right] \\ & \times K_{\bar{P},\bar{P}'}^\mu \\ & \times \left[G_{0\bar{P}'} - i G_{0\bar{P}'} \left(V_R^{(3)} + \bar{K}_{\bar{P}'}^{(2)} - V_{\bar{P}'}^{\text{eff}(1)} \right) G_{0\bar{P}'} \right], \end{aligned} \quad (25)$$

which we expand to the same order in the residual kernel as the effective kernel V_M^{eff} used in the Salpeter equation, *i.e.* up to the first order

$$\mathcal{K}_{\bar{P},\bar{P}'}^\mu = \mathcal{K}_{\bar{P},\bar{P}'}^{\mu(0)} + \mathcal{K}_{\bar{P},\bar{P}'}^{\mu(1)} + \text{higher orders.} \quad (26)$$

Here the 0-th-order contribution is defined as

$$\mathcal{K}_{\bar{P},\bar{P}'}^{\mu(0)} = G_{0\bar{P}} K_{\bar{P},\bar{P}'}^{\mu(0)} G_{0\bar{P}'} \quad (27)$$

and reads explicitly

$$\begin{aligned} \mathcal{K}_{\bar{P},\bar{P}'}^{\mu(0)}(p_\xi, p_\eta, p'_\xi, p'_\eta) = & S_F^1 \left(\frac{1}{3}\bar{P} + p_\xi + \frac{1}{2}p_\eta \right) \otimes S_F^2 \left(\frac{1}{3}\bar{P} - p_\xi + \frac{1}{2}p_\eta \right) \\ & \otimes S_F^3 \left(\frac{1}{3}\bar{P} - p_\eta \right) \hat{q} \gamma^\mu S_F^3 \left(\frac{1}{3}\bar{P}' - p'_\eta \right) \\ & \times (2\pi)^4 \delta^{(4)}(p_\xi - p'_\xi) (2\pi)^4 \delta^{(4)} \left(\frac{2}{3}(\bar{P} - \bar{P}') + p_\eta - p'_\eta \right) \\ & + \text{corresponding photon couplings to quarks 1 and 2.} \end{aligned} \quad (28)$$

The 1st-order contribution reads

$$\begin{aligned} \mathcal{K}_{\bar{P},\bar{P}'}^{\mu(1)} = & G_{0\bar{P}} K_{\bar{P},\bar{P}'}^{\mu(1)} G_{0\bar{P}'} \\ & - i G_{0\bar{P}} K_{\bar{P},\bar{P}'}^{\mu(0)} G_{0\bar{P}'} \left(V_R^{(3)} + \bar{K}_{\bar{P}'}^{(2)} - V_{\bar{P}'}^{\text{eff}(1)} \right) G_{0\bar{P}'} \\ & - i G_{0\bar{P}} \left(V_R^{(3)} + \bar{K}_{\bar{P}}^{(2)} - V_{\bar{P}}^{\text{eff}(1)} \right) G_{0\bar{P}} K_{\bar{P},\bar{P}'}^{\mu(0)} G_{0\bar{P}'}. \end{aligned} \quad (29)$$

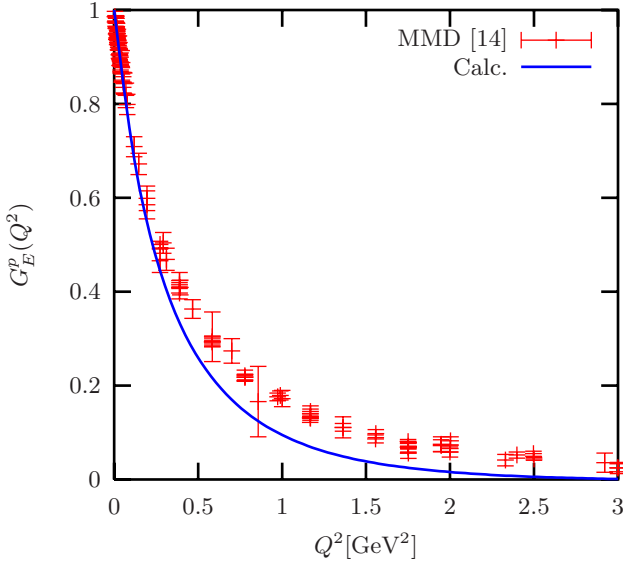


Fig. 1. The electric form factor of the proton. Data are taken from the compilation of P. Mergell *et al.* (MMD) [14].

Due to the complexity of the first-order contribution $\mathcal{K}_{\bar{P},\bar{P}'}^{\mu(1)}$ to the current matrix element we neglected so far this term in our calculations and took only the 0-th-order term $\mathcal{K}_{\bar{P},\bar{P}'}^{\mu(0)}$ into account. We should mention at this point that in the static limit $\bar{P} = \bar{P}' = M \equiv (M, \mathbf{0})$ the first-order term does not contribute to the normalization of the charge as it vanishes for the time component of the current, *i.e.*

$$\bar{\Gamma}_M^A \mathcal{K}_{M,M}^{0(1)} \Gamma_M^A = 0, \quad (30)$$

while the 0-th-order term alone gives the correct normalization due to the normalization condition of the Salpeter amplitudes. Neglecting $\mathcal{K}_{\bar{P},\bar{P}'}^{\mu(1)}$ and setting the incoming baryon into the rest frame, *i.e.* $\bar{P}' = M \equiv (M, \mathbf{0})$, we then obtain for momentum transfer $q := \bar{P} - \bar{P}'$

$$\begin{aligned} \langle \bar{P} | j^\mu(0) | M \rangle &\simeq -\bar{\Gamma}_{\bar{P}}^A \mathcal{K}_{\bar{P},M}^{\mu(0)} \Gamma_M^A = \\ &-3 \int \frac{d^4 p_\xi}{(2\pi)^4} \frac{d^4 p_\eta}{(2\pi)^4} \bar{\Gamma}_{\bar{P}}^A \left(p_\xi, p_\eta - \frac{2}{3}q \right) \\ &\times S_F^1 \left(\frac{1}{3}M + p_\xi + \frac{1}{2}p_\eta \right) \otimes S_F^2 \left(\frac{1}{3}M - p_\xi + \frac{1}{2}p_\eta \right) \\ &\otimes S_F^3 \left(\frac{1}{3}M - p_\eta + q \right) \hat{q} \gamma^\mu S_F^3 \left(\frac{1}{3}M - p_\eta \right) \Gamma_M^A(\mathbf{p}_\xi, \mathbf{p}_\eta). \end{aligned}$$

This is the final expression for the current matrix elements which we use for the computation of form factors in the next section.

3 Electroweak form factors of the nucleon

On the basis of the theoretical considerations of the preceding section we compute the current matrix elements

$$\langle N, \bar{P}, \lambda | j_\mu^{E,A}(0) | N, \bar{P}', \lambda' \rangle, \quad (31)$$

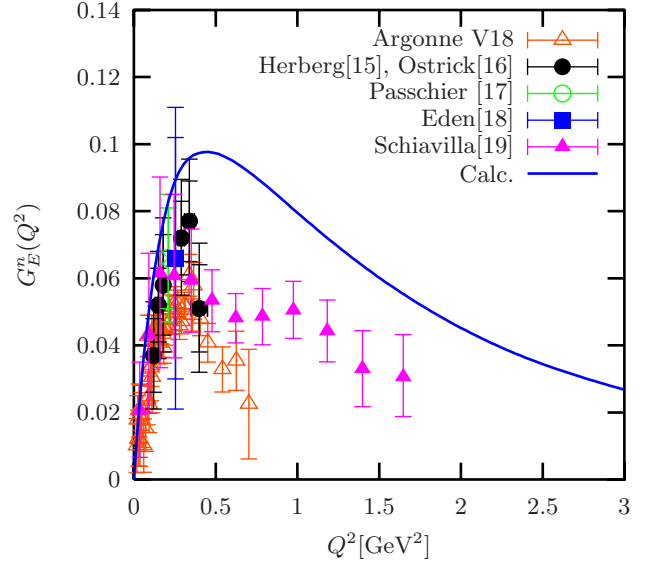


Fig. 2. The electric form factor of the neutron.

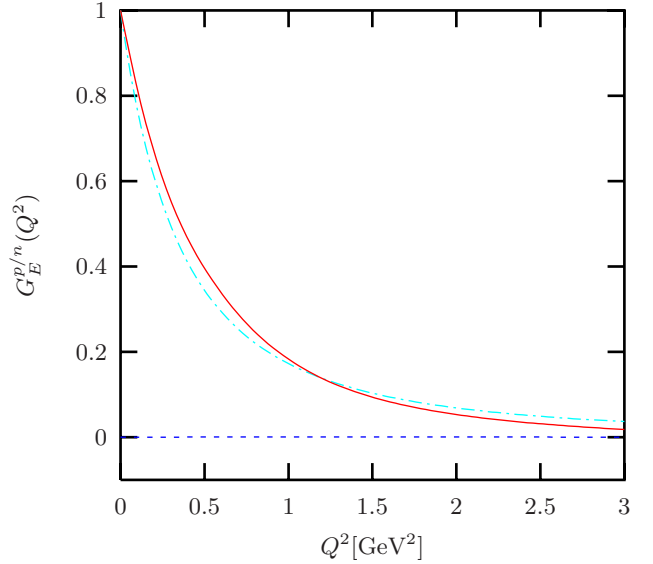


Fig. 3. The electric form factor of the proton (solid line) and neutron (dashed line) calculated without the instanton-induced residual interaction compared with the experimental dipole shape G_D (dash-dotted line).

for a nucleon state $|N, \bar{P}, \lambda\rangle$ with momentum \bar{P} and helicity λ , where $j_\mu^{E,A}(0)$ is the electromagnetic or axial current operator

$$j_\mu^E(x) := \bar{\Psi}(x) \hat{q} \gamma_\mu \Psi(x); \quad j_\mu^A(x) := \bar{\Psi}(x) \tau^+ \gamma_\mu \gamma^5 \Psi(x). \quad (32)$$

They determine the electric, magnetic and axial form factors according to ($Q^2 = -q^2$)

$$G_E^N(Q^2) := \frac{j_0^N(Q^2)}{\sqrt{4M^2 + Q^2}}, \quad G_M^N(Q^2) := \frac{j_+^N(Q^2)}{2\sqrt{Q^2}}, \quad (33)$$

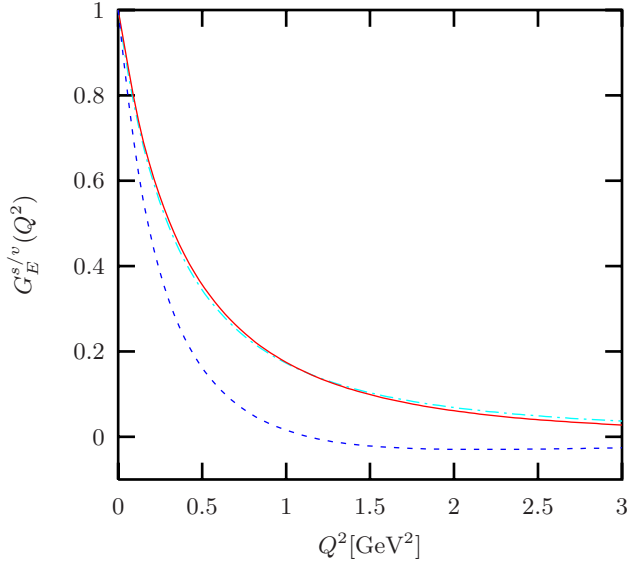


Fig. 4. The electric isoscalar (solid line) and isovector (dashed line) form factors for the nucleon compared with the experimental dipole shape G_D (dash-dotted line).

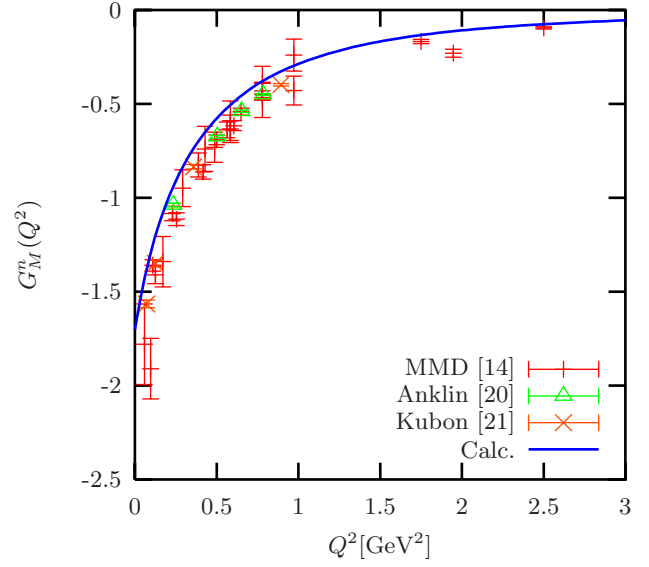


Fig. 6. The magnetic form factor of the neutron compared with (MMD) [14] and new data from MAMI [20,21].

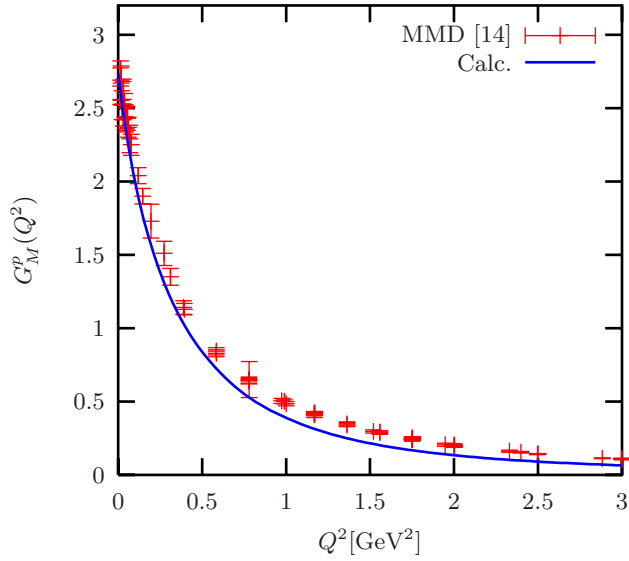


Fig. 5. The magnetic form factor of the proton. Data are taken from the compilation of P. Mergell *et al.* (MMD) [14].

where

$$j_0^N(0) := \left\langle N, \bar{P}, \frac{1}{2} \left| j_0^E(0) \right| N, \bar{P}', \frac{1}{2} \right\rangle, \quad (34)$$

$$j_+^N(0) := \left\langle N, \bar{P}, \frac{1}{2} \left| j_1^E(0) \right| N, \bar{P}', -\frac{1}{2} \right\rangle + i \left\langle N, \bar{P}, \frac{1}{2} \left| j_2^E(0) \right| N, \bar{P}', -\frac{1}{2} \right\rangle \quad (35)$$

for the electromagnetic form factors and

$$G_A(Q^2) := \frac{j_A^+(Q^2)}{\sqrt{4M^2 + Q^2}}, \quad (36)$$

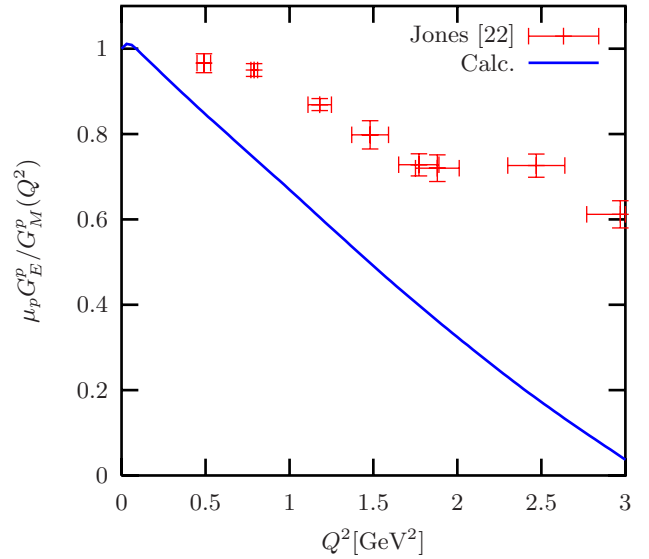


Fig. 7. The ratio $\mu_p G_E^p / G_M^p$ compared with the new JLab data [22].

with

$$j_A^+(Q^2) := \left\langle p, \bar{P}, \frac{1}{2} \left| j_1^A(0) \right| n, \bar{P}', -\frac{1}{2} \right\rangle + i \left\langle p, \bar{P}, \frac{1}{2} \left| j_2^A(0) \right| n, \bar{P}', -\frac{1}{2} \right\rangle \quad (37)$$

for the axial one. The normalization of the form factors is such that the static magnetic moments and the axial coupling are given by

$$\mu_M := G_M(Q^2 = 0), \quad g_A := G_A(Q^2 = 0). \quad (38)$$

The result for the proton electric form factor is shown in fig. 1. The form factor obviously falls off too rapidly.

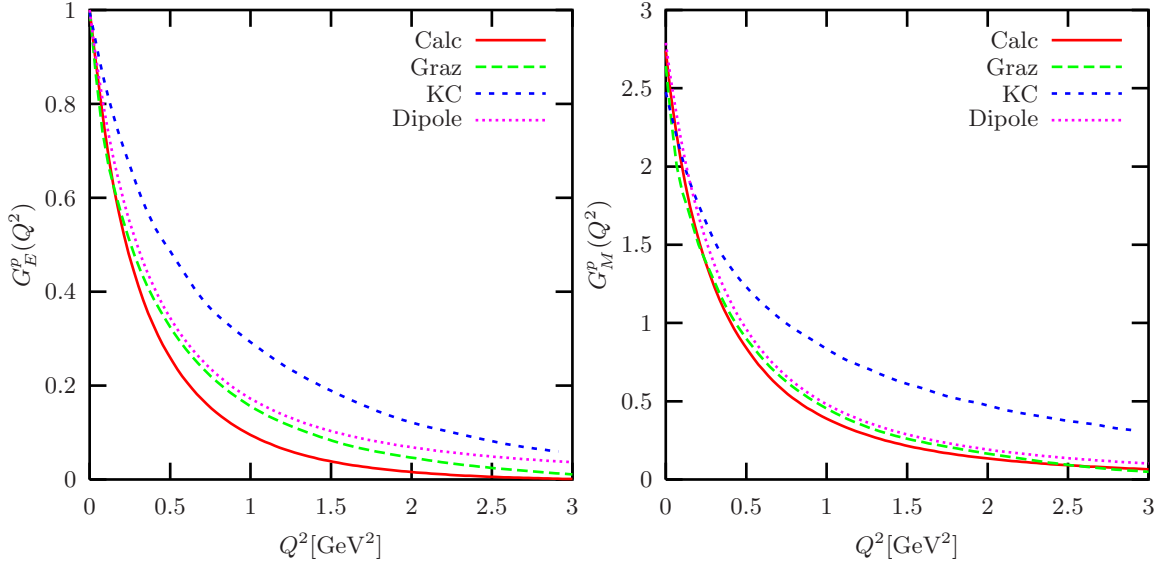


Fig. 8. The electric and magnetic form factor of the proton compared to the results of Wagenbrunn *et al.* (Graz) [4], Keister and Capstick (KC) [23] and the dipole fit to the data.

The electric form factor of the neutron, shown in fig. 2, rises sharply; the high- Q^2 behaviour of our theoretical prediction is still acceptable. The sharp rise is in qualitative agreement with more recent data, but our result overshoots the experimental values. The rapid fall-off of the proton form factor and the sharp rise of the neutron form factor result from the action of the 't Hooft interaction. To demonstrate this we show in fig. 3 the result of a calculation with the confinement force alone (which, of course, will not yield a satisfactory spectrum).

A closer look at the results shows that it is the behaviour of the isovector form factor $G_E^v := G_E^p - G_E^n$, which is responsible for the disagreement with the empirical data. The isoscalar form factor $G_E^s := G_E^p + G_E^n$ shows indeed even a perfect dipole behaviour (see fig. 4), consistent with the experimental parametrization $G_D(Q^2) = (1 + Q^2/0.71 \text{ GeV}^2)^{-2}$. We want to note in addition that the neutron form factor, which we have computed, still has a chance to agree with experiment, because the extraction from deuteron scattering is not free of ambiguities. A recent paper [24], which treats this problem, produces in fact neutron form factors in qualitative agreement with our results.

In figs. 5 and 6 we show our results for the magnetic form factors of proton and neutron. Obviously we describe the data very well. This is interesting in so far as we induce by 't Hooft's force strong correlations in the amplitudes, which in standard non-relativistic quark models spoil the symmetry of the wave function and destroy therefore the classical $SU(6)$ results for magnetic moments. We believe that the correct relativistic boosting of our amplitudes is responsible for the good agreement with the data. For comparison we have calculated the magnetic moment of the proton omitting the boost (as in

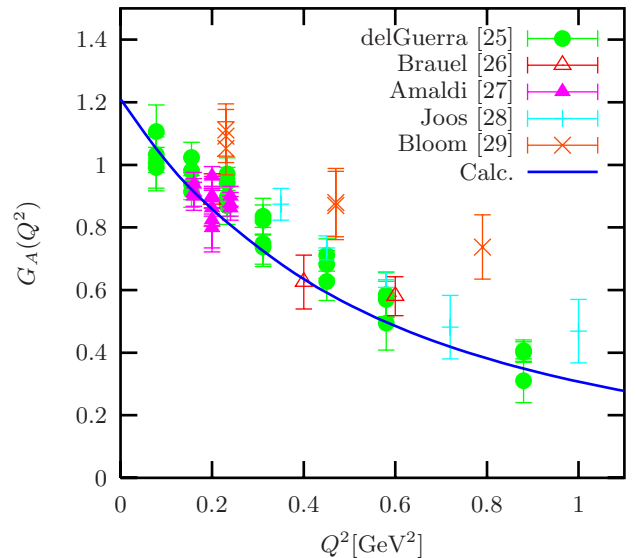


Fig. 9. The axial form factor of the nucleon. Data are taken from the compilation of V. Bernard *et al.* [31].

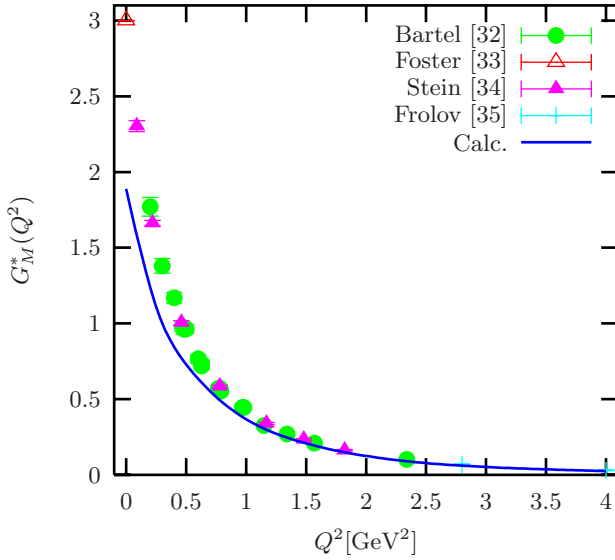
non-relativistic calculations). The value drops in fact by the order of one magneton.

Very recently the ratio $\mu_p G_E^p / G_M^p$ has been measured with high accuracy at Jefferson Lab [22]. The data show a monotonical, almost linear decrease with increasing Q^2 indicating that the electric form factor of the proton decreases significantly faster than the dipole G_D , which is in qualitative agreement with our results (see fig. 7). But due to the rapid fall-off of G_E^p the ratio is strongly underestimated in our model for high Q^2 .

In fig. 8 we compare our results for the electric and magnetic form factor of the proton with the predictions

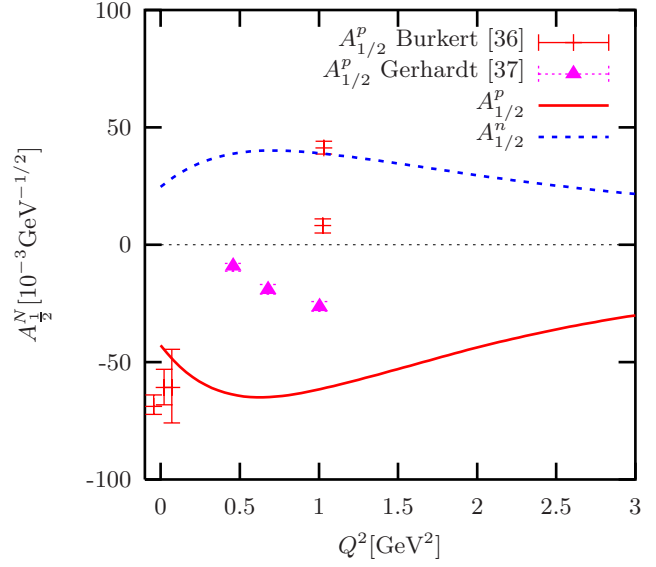
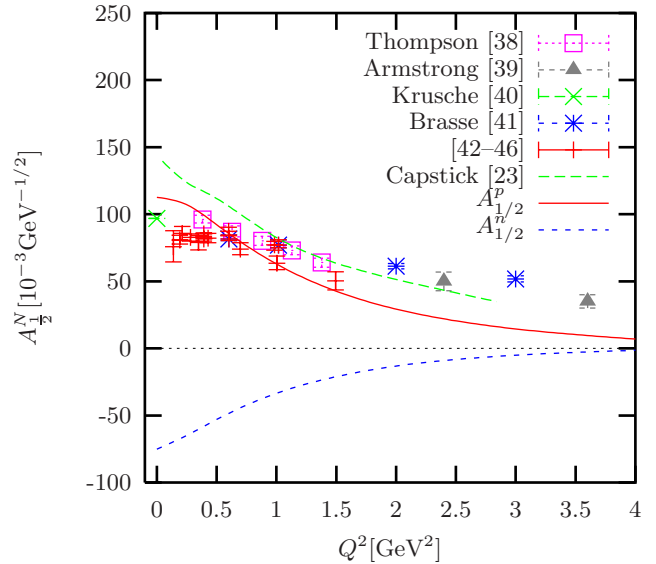
Table 1. Static properties of the nucleon.

	Calc.	Exp.	
μ_p	$2.74 \mu_N$	$2.793 \mu_N$	[30]
μ_n	$-1.70 \mu_N$	$-1.913 \mu_N$	[30]
$\sqrt{\langle r^2 \rangle_E^p}$	0.82 fm	0.847 fm	[14]
$\langle r^2 \rangle_E^n$	0.11 fm^2	$0.113 \pm 0.004 \text{ fm}^2$	[14]
$\sqrt{\langle r^2 \rangle_M^p}$	0.91 fm	0.836 fm	[14]
$\sqrt{\langle r^2 \rangle_M^n}$	0.86 fm	0.889 fm	[14]
g_A	1.21	1.2670 ± 0.0035	[30]
$\sqrt{\langle r^2 \rangle_A}$	0.62 fm	$0.61 \pm 0.01 \text{ fm}$	[31]

**Fig. 10.** $\Delta(1232)$ magnetic transition form factor.

of the Goldstone-boson-exchange model of Wagenbrunn *et al.* [4] and the light-front calculation of Keister and Capstick [23] using the wave functions of the relativized quark model of Capstick and Isgur [2]. In addition the phenomenological dipole fit of the experimental data is shown to facilitate the comparison with experiment. We have chosen these two alternative models because for both of them more form factor calculations (hyperons and transition form factors) are available or could be done in principle. (We apologize that for lack of space we do not show here the work of other authors.) Both alternative models have the problem that a basically non-covariant calculation based on the Schrödinger equation has to be relativized by an additional recipe introduced *ad hoc*. In our model such a necessity does not show up, because the formalism is dictated by a covariant field theory approach. It is therefore quite satisfactory, that our approach can compete quantitatively with the older work.

Figure 9 shows our result for the axial form factor in comparison with the experimental data, which show in

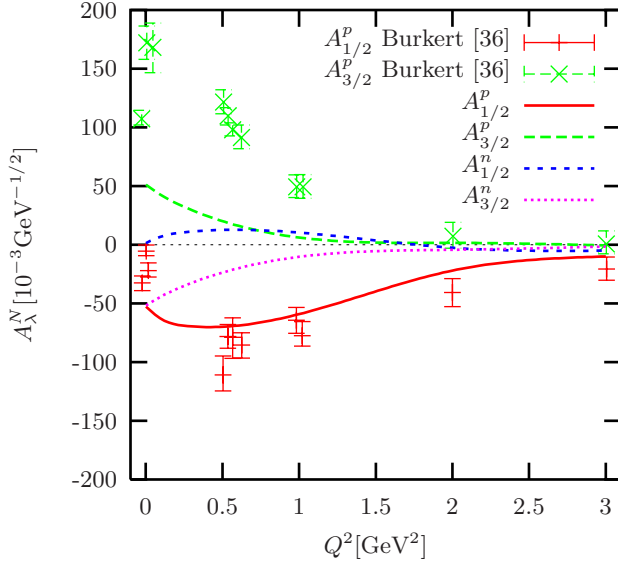
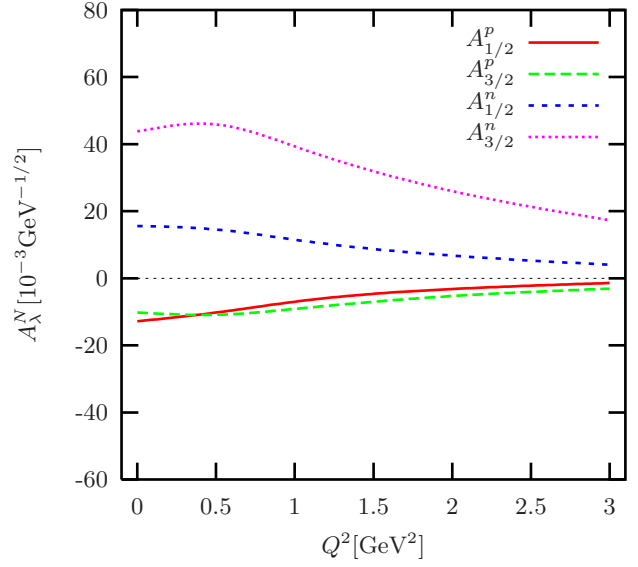
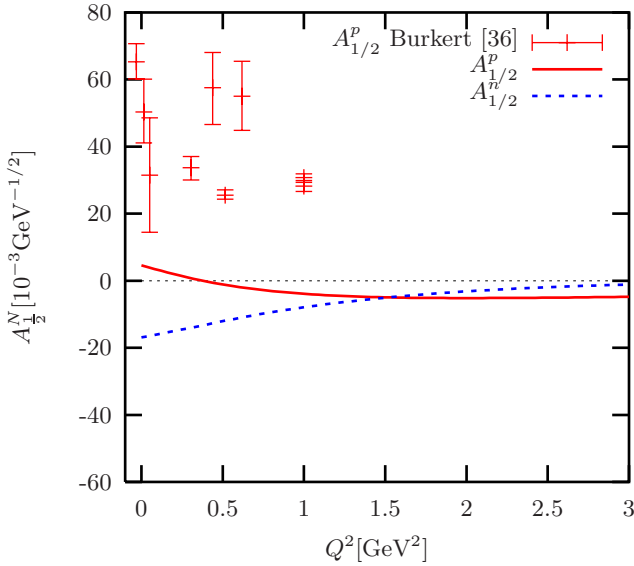
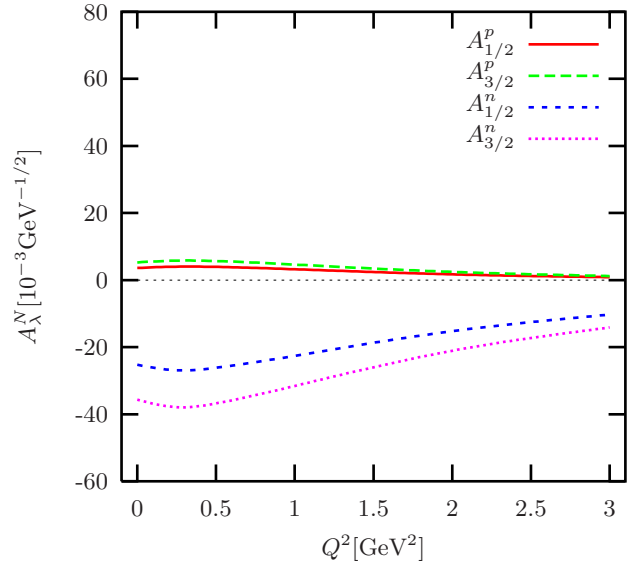
**Fig. 11.** $P_{11}(1440)$ electroexcitation helicity amplitudes.**Fig. 12.** $S_{11}(1535)$ electroexcitation helicity amplitudes.

fact large deviations between several experimental groups. Our theoretical results agree, however, very well with the more recent experimental work.

We conclude this section with a table of static electroweak constants of the nucleon (table 1). Apparently we achieved a reasonably good agreement with the common experimental values.

4 Transition form factors

The nucleon- Δ transition form factor is intensively studied since many years. A long-standing problem is the smallness of this quantity at low Q^2 in quark model calculations, which can only be cured by hybrid models with

Fig. 13. $D_{13}(1520)$ electroexcitation helicity amplitudes.Fig. 15. $D_{13}(1700)$ electroexcitation helicity amplitudes.Fig. 14. $S_{11}(1650)$ electroexcitation helicity amplitudes.Fig. 16. $D_{15}(1675)$ electroexcitation helicity amplitudes.

a mesonic cloud around the nucleon [47,48]. Our result, compared to the experimental data, is shown in fig. 10. We see that at small Q^2 we do not cure this old quark model prediction and that our form factor remains too small. The Q^2 behaviour above 1 GeV^2 , however, is correct.

The results for the transition form factors of the second and third resonance region are presented in the form of the helicity amplitudes A_λ^p and A_λ^n for proton and neutron targets, respectively, defined by

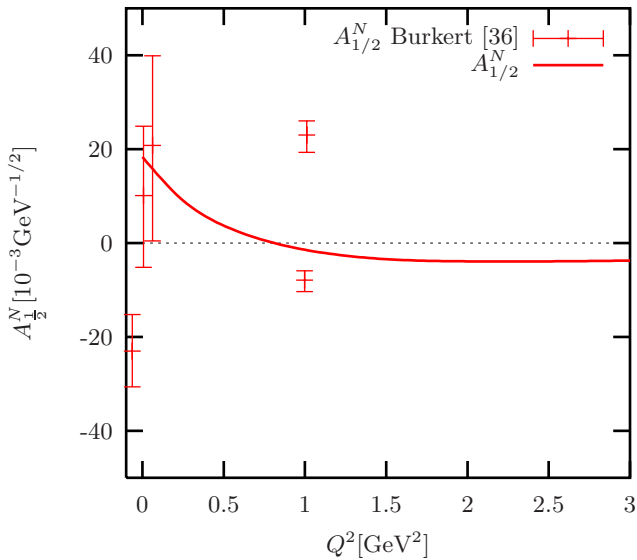
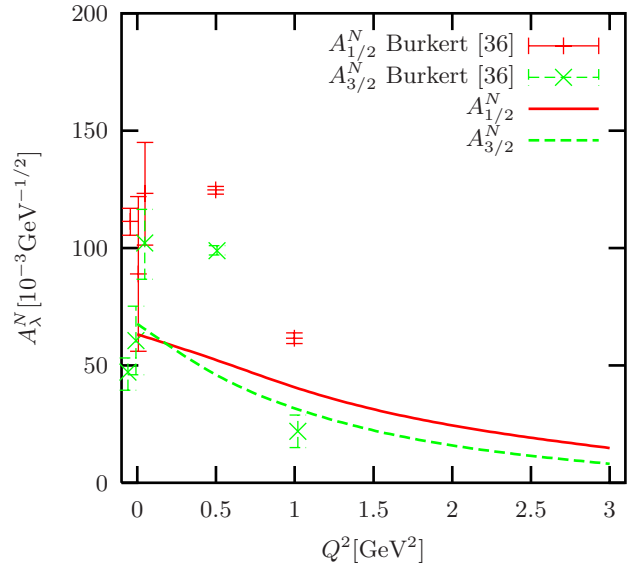
$$A_\lambda^N := C \langle N^*, \bar{P}, \lambda | j_1^E(0) + i j_2^E(0) | N, \bar{P}', \lambda - 1 \rangle \quad (39)$$

with $C := \sqrt{\frac{\pi\alpha}{2M_{N^*}(M_{N^*}^2 - M_N^2)}}$ following [49]. For the Roper resonance $P_{11}(1440)$ (see fig. 11) experimental data are unfortunately contradicting each other, because the ex-

traction from pion photoproduction is strongly model dependent. The experimental situation is much better for the $S_{11}(1535)$ and $D_{13}(1520)$, though not completely conclusive. In fig. 12 we show the available experimental data for the S_{11} together with our result and the result of a quark model calculation by Capstick [23]. We see that our model works better at low Q^2 but our form factor possibly drops too fast. The helicity amplitude $A_{1/2}^p$ for $D_{13}(1520)$ (see fig. 13) is well reproduced, but the amplitude $A_{3/2}^p$ seems to be too small even at the photon point. To complete our results for the $1\hbar\omega$ shell we show the helicity amplitudes for $S_{11}(1650)$, $D_{13}(1700)$ and $D_{15}(1675)$ in figs. 14, 15 and 16 and for the Δ -resonances $S_{31}(1620)$ and $D_{33}(1700)$ in figs. 17 and 18. Experimental data to compare with, taken

Table 2. Photon couplings.

State	Calc.	KI [50]	Exp. [30]	Calc.	KI [50]	Exp. [30]	State	Calc.	KI [50]	Exp. [30]			
$S_{11}(1535)$	$A_{\frac{1}{2}}^p$	113	147	90 ± 30	$A_{\frac{1}{2}}^n$	-75	-119	-46 ± 27	$P_{33}(1232)$	$A_{\frac{1}{2}}^N$	-89	-103	-135 ± 6
$S_{11}(1650)$	$A_{\frac{1}{2}}^p$	5	88	53 ± 16	$A_{\frac{1}{2}}^n$	-16	-35	-15 ± 21		$A_{\frac{3}{2}}^N$	-152	-179	-255 ± 8
$D_{13}(1520)$	$A_{\frac{1}{2}}^p$	-53	-23	-24 ± 9	$A_{\frac{1}{2}}^n$	1	-45	-59 ± 9	$S_{31}(1620)$	$A_{\frac{1}{2}}^N$	18	59	27 ± 11
	$A_{\frac{3}{2}}^p$	51	128	166 ± 5	$A_{\frac{3}{2}}^n$	-52	-122	-139 ± 11	$D_{33}(1700)$	$A_{\frac{1}{2}}^N$	63	100	104 ± 15
$D_{13}(1700)$	$A_{\frac{1}{2}}^p$	-13	-7	-18 ± 13	$A_{\frac{1}{2}}^n$	16	-15	0 ± 50		$A_{\frac{3}{2}}^N$	68	105	85 ± 22
	$A_{\frac{3}{2}}^p$	-10	11	-2 ± 24	$A_{\frac{3}{2}}^n$	-42	-76	-3 ± 44					
$D_{15}(1675)$	$A_{\frac{1}{2}}^p$	4	12	19 ± 8	$A_{\frac{1}{2}}^n$	-25	-37	-43 ± 12					
	$A_{\frac{3}{2}}^p$	5	16	15 ± 9	$A_{\frac{3}{2}}^n$	-33	-53	-58 ± 13					
$P_{11}(1440)$	$A_{\frac{1}{2}}^p$	-48	-24	-65 ± 4	$A_{\frac{1}{2}}^n$	27	16	40 ± 10					

**Fig. 17.** $S_{31}(1620)$ electroexcitation helicity amplitude.**Fig. 18.** $D_{33}(1700)$ electroexcitation helicity amplitudes.

from [36], are again quite contradictory but new measurements at Jefferson Laboratory are in progress.

The photon couplings of all these resonances are summarized in table 2, compared with the results of the non-relativistic model of Koniuk and Isgur [50]. With the exceptions discussed just before, they agree quite well with the data. Our results for the second and third resonance region are therefore quite satisfactory; because of the total lack of experimental data we stop, however, our investigation of form factors at this point, though we could in principle continue with higher resonances.

5 Conclusion

On the basis of the Bethe-Salpeter equation we have computed nucleon form factors and photon transition form

factors of baryons up to the third resonance region. Our results are in quantitative agreement with the existent experimental data, but need further experimental verification. Our fully relativistic treatment proved to be absolutely necessary to reach these results; in addition we were able to demonstrate that our dynamical assumptions about the effective quark forces at least do not lead to contradictions. In future work higher orders of the effective kernels V_M^{eff} and $\mathcal{K}_{P,P'}^\mu$, neglected so far will be taken into account. So far we did not find strong indications that the concept of constituent quarks fails completely at the energies considered. There is of course room for improvements, *e.g.* sea quark admixtures or pion cloud effects as used in some hybrid models. We have made no efforts in this direction, because our goal is to explore the concept of constituent quarks at higher energies in order to find

out when it really fails. In the same spirit we are now performing similar calculations of strange baryon properties and strong two-body decays of baryon resonances.

We want to thank our colleagues U. Meißner, E. Klempt, F. Klein, B. Schoch, W. Pfeil, V.V. Anisovich, A. Sarantsev, H. Schmieden and S. Capstick for many helpful discussions and useful hints. The financial aid of the Deutsche Forschungsgemeinschaft is gratefully acknowledged.

Appendix A. Reconstruction of the Bethe-Salpeter amplitude

In our first paper [6] we demonstrated how, under assumptions (5) and (6), the Bethe-Salpeter equation (2)

$$\chi_M = -i G_{0M} \left(V^{(3)} + \overline{K}_M^{(2)} \right) \chi_M, \quad (\text{A.1})$$

can be reduced (in the rest frame of the baryon) to a Salpeter equation for the (projected) Salpeter amplitude

$$\begin{aligned} \Phi_M^A(\mathbf{p}_\xi, \mathbf{p}_\eta) &:= \\ \Lambda(\mathbf{p}_\xi, \mathbf{p}_\eta) &\int \frac{dp_\xi^0}{2\pi} \frac{dp_\eta^0}{2\pi} \chi_M((p_\xi^0, \mathbf{p}_\xi), (p_\eta^0, \mathbf{p}_\eta)). \end{aligned} \quad (\text{A.2})$$

Here

$$\begin{aligned} \Lambda(\mathbf{p}_\xi, \mathbf{p}_\eta) &:= \Lambda^{+++}(\mathbf{p}_\xi, \mathbf{p}_\eta) + \Lambda^{---}(\mathbf{p}_\xi, \mathbf{p}_\eta) \\ &= \Lambda_1^+(\mathbf{p}_1) \otimes \Lambda_2^+(\mathbf{p}_2) \otimes \Lambda_3^+(\mathbf{p}_3) \\ &\quad + \Lambda_1^-(\mathbf{p}_1) \otimes \Lambda_2^-(\mathbf{p}_2) \otimes \Lambda_3^-(\mathbf{p}_3) \end{aligned} \quad (\text{A.3})$$

is a projector on purely positive-energy and negative-energy Dirac spinors. To perform the reduction we split the integral kernel $K_M = V^{(3)} + \overline{K}_M^{(2)}$ of the Bethe-Salpeter equation into two parts

$$K_M = V_A^{(3)} + \left(V_R^{(3)} + \overline{K}_M^{(2)} \right). \quad (\text{A.4})$$

The first part $V_A^{(3)} := \overline{\Lambda} V^{(3)} \Lambda$ of the kernel (with $\overline{\Lambda} := \gamma^0 \otimes \gamma^0 \otimes \gamma^0$) is the particular contribution of the instantaneous three-body potential $V^{(3)}$ which couples to purely positive-energy and negative-energy components only. The second, residual part $V_R^{(3)} + \overline{K}_M^{(2)}$ is the sum of the retarded two body contribution $\overline{K}_M^{(2)}$ and the remaining part $V_R^{(3)} := V^{(3)} - V_A^{(3)}$ of $V^{(3)}$ that also couples to the mixed energy components. Putting the difficult residual contribution into the resolvent

$$\mathcal{G}_M = G_{0M} - i G_{0M} \left[V_R^{(3)} + \overline{K}_M^{(2)} \right] \mathcal{G}_M, \quad (\text{A.5})$$

the Bethe-Salpeter equation can be written in the form

$$\chi_M = -i \mathcal{G}_M V_A^{(3)} \Phi_M^A. \quad (\text{A.6})$$

This form, firstly, gives a prescription of how to reconstruct the full Bethe-Salpeter amplitude χ_M from the

Salpeter amplitude Φ_M^A and, secondly, is suitable for the reduction to the Salpeter equation as $V_A^{(3)}$ is instantaneous. We obtained

$$\Phi_M^A = -i \langle G_{0M} \rangle \left[V_A^{(3)} + V_M^{\text{eff}} \right] \Phi_M^A, \quad (\text{A.7})$$

where the brackets $\langle \rangle$ denote the six-dimensional reduction

$$\begin{aligned} \langle A \rangle(\mathbf{p}_\xi, \mathbf{p}_\eta; \mathbf{p}'_\xi, \mathbf{p}'_\eta) &:= \\ &\int \frac{dp_\xi^0}{2\pi} \frac{dp_\eta^0}{2\pi} \int \frac{dp'_\xi^0}{2\pi} \frac{dp'_\eta^0}{2\pi} A(p_\xi, p_\eta; p'_\xi, p'_\eta) \end{aligned} \quad (\text{A.8})$$

of any eight-dimensional six-point function A and V_M^{eff} (with the property $\overline{\Lambda} V_M^{\text{eff}} = V_M^{\text{eff}} \Lambda = V_M^{\text{eff}}$) is an additional instantaneous three-body kernel which effectively parameterizes the effects of the retarded two-body forces. The latter is defined as the irreducible kernel for the resolvent $\langle \mathcal{G}_M \rangle_A := \Lambda \langle \mathcal{G}_M \rangle \overline{\Lambda}$, where the irreducible is understood with respect to $\langle G_{0M} \rangle$, *i.e.*

$$\langle \mathcal{G}_M \rangle_A \stackrel{!}{=} \langle G_{0M} \rangle - i \langle G_{0M} \rangle V_M^{\text{eff}} \langle \mathcal{G}_M \rangle_A. \quad (\text{A.9})$$

To determine this quasi-potential we expanded it in powers k of the residual kernel $V_R^{(3)} + \overline{K}_M^{(2)}$, *i.e.*

$$V_M^{\text{eff}} = \sum_{k=1}^{\infty} V_M^{\text{eff}(k)}. \quad (\text{A.10})$$

In ref. [6] we derived a generic formula to calculate the terms $V_M^{\text{eff}(k)}$ of the series to arbitrary orders. In practice, however, we have to approximate the effective kernel V_M^{eff} , which consists of an infinite number of terms. A systematic approximation is now given by truncating the series (A.10) at some finite order $k < \infty$, *i.e.*

$$V_M^{\text{eff}} \simeq V_M^{\text{eff}(1)} + V_M^{\text{eff}(2)} + \dots + V_M^{\text{eff}(k)}, \quad (\text{A.11})$$

thus yielding an approximation of the Salpeter amplitude $\Phi_M^A \simeq \Phi_M^{A(k)}$ by the solution of

$$\Phi_M^{A(k)} = -i \langle G_{0M} \rangle \left(V_A^{(3)} + \sum_{i=1}^k V_M^{\text{eff}(i)} \right) \Phi_M^{A(k)}. \quad (\text{A.12})$$

For the calculation of transition matrix elements we need the full Bethe-Salpeter amplitude which (if V_M^{eff} and Φ_M^A are known exactly) can be reconstructed by the prescription (A.6) via the Green's function \mathcal{G}_M . However, the truncation of the Salpeter equation has the consequence that the relation (A.6) does not hold for $\Phi_M^{A(k)}$. To be consistent we need an approximation of this reconstruction formula that corresponds to the approximation (A.11) of the effective kernel. In other words, we require the corresponding k -th-order approximation $\chi_M^{(k)}$ of the Bethe-Salpeter amplitude χ_M to be such that its reduction according to eq. (A.2) yields the k -th-order approximation $\Phi_M^{A(k)}$ of the

Salpeter amplitude. Here we want to show that a consistent prescription for an approximated reconstruction of the Bethe-Salpeter amplitude can indeed be found. To this end, we recast the Bethe-Salpeter and Salpeter equation into a more convenient form. We start with the exact Bethe-Salpeter equation (A.1) and isolate the instantaneous part $V_A^{(3)} + \sum_{i=1}^k V_M^{\text{eff}(i)}$ of the kernel which enters in the k -th-order approximation of the Salpeter equation (A.12):

$$\chi_M = -i G_{0M} \left[\left(V_A^{(3)} + \sum_{i=1}^k V_M^{\text{eff}(i)} \right) + \left(\overline{K}_M^{(2)} + V_R^{(3)} - \sum_{i=1}^k V_M^{\text{eff}(i)} \right) \right] \chi_M. \quad (\text{A.13})$$

The exact Bethe-Salpeter equation can then be rewritten as follows:

$$\chi_M = -i \mathcal{G}_M^{R,k} \left(V_A^{(3)} + \sum_{i=1}^k V_M^{\text{eff}(i)} \right) \chi_M \quad (\text{A.14})$$

$$= -i \mathcal{G}_M^{R,k} \left(V_A^{(3)} + \sum_{i=1}^k V_M^{\text{eff}(i)} \right) \Phi_M^A, \quad (\text{A.15})$$

giving a reconstruction formula for χ_M from Φ_M^A , which is equivalent to eq. (A.6) but better suited to formulate our approximation for the full amplitude. Here a new residual propagator $\mathcal{G}_M^{R,k}$ appears which describes the propagation of the three quarks via the second part of the kernel in (A.13) and which is defined by the integral equation

$$\mathcal{G}_M^{R,k} = G_{0M} - i G_{0M} \left(\overline{K}_M^{(2)} + V_R^{(3)} - \sum_{i=1}^k V_M^{\text{eff}(i)} \right) \mathcal{G}_M^{R,k}. \quad (\text{A.16})$$

Performing the reduction of eq. (A.15) —*i.e.* the integration over the p_ξ^0, p_η^0 -coordinates and the multiplication with the projector Λ — we obtain the (still exact) Salpeter equation in the form

$$\Phi_M^A = -i \langle \mathcal{G}_M^{R,k} \rangle_\Lambda \left[V_A^{(3)} + \sum_{i=1}^k V_M^{\text{eff}(i)} \right] \Phi_M^A, \quad (\text{A.17})$$

where the reduced (and projected) Green's function defined by $\langle \mathcal{G}_M^{R,k} \rangle_\Lambda := \Lambda \langle \mathcal{G}_M^{R,k} \rangle \overline{\Lambda}$ obeys

$$\langle \mathcal{G}_M^{R,k} \rangle_\Lambda = \langle G_{0M} \rangle - i \langle G_{0M} \rangle \sum_{i=k+1}^{\infty} V_M^{\text{eff}(i)} \langle \mathcal{G}_M^{R,k} \rangle_\Lambda. \quad (\text{A.18})$$

The crucial point is now that the kernel appearing in this integral equation is obviously at least of $(k+1)$ -th order of the residual kernel $V_R^{(3)} + \overline{K}_M^{(2)}$. In particular the Neumann series of $\langle \mathcal{G}_M^{R,k} \rangle_\Lambda$ consists, apart from the 0-th-order term $\langle G_{0M} \rangle$, only of terms of order $> k$. In other words, if we expand the propagator $\mathcal{G}_M^{R,k}$, similar to the effective kernel

V_M^{eff} , in powers of the residual kernel $V_R^{(3)} + \overline{K}_M^{(2)}$, *i.e.*

$$\mathcal{G}_M^{R,k} = \sum_{i=0}^{\infty} \mathcal{G}_M^{R,k(i)} \quad (\text{A.19})$$

and consider only terms up to the k -th order, we find

$$\left\langle \sum_{i=0}^k \mathcal{G}_M^{R,k(i)} \right\rangle_\Lambda := \Lambda \left\langle \sum_{i=0}^k \mathcal{G}_M^{R,k(i)} \right\rangle \overline{\Lambda} = \langle G_{0M} \rangle. \quad (\text{A.20})$$

This result now allows to state an appropriate approximation of the full Bethe-Salpeter equation which is consistent with the Salpeter equation (A.12): replacing in the exact Bethe-Salpeter equation (A.14) the propagator $\mathcal{G}_M^{R,k}$ by its expansion (A.19) up to the order k

$$\mathcal{G}_M^{R,k} \longrightarrow \sum_{i=0}^k \mathcal{G}_M^{R,k(i)}, \quad (\text{A.21})$$

we obtain an approximation of the Salpeter amplitude $\chi_M \simeq \chi_M^{(k)}$ by the solution of the approximated Bethe-Salpeter equation

$$\chi_M^{(k)} = -i \sum_{i=0}^k \mathcal{G}_M^{R,k(i)} \left(V_A^{(3)} + \sum_{i=1}^k V_M^{\text{eff}(i)} \right) \chi_M^{(k)}. \quad (\text{A.22})$$

Then, the corresponding reduced amplitude

$$\Phi_M^{A(k)}(\mathbf{p}_\xi, \mathbf{p}_\eta) := \Lambda(\mathbf{p}_\xi, \mathbf{p}_\eta) \int \frac{dp_\xi^0}{2\pi} \frac{dp_\eta^0}{2\pi} \chi_M^{(k)}((p_\xi^0, \mathbf{p}_\xi), (p_\eta^0, \mathbf{p}_\eta)), \quad (\text{A.23})$$

is indeed the solution of the approximated Salpeter equation (A.12) and $\chi_M^{(k)}$ can be reconstructed from $\Phi_M^{A(k)}$ according to

$$\chi_M^{(k)} = -i \sum_{i=0}^k \mathcal{G}_M^{R,k(i)} \left(V_A^{(3)} + \sum_{i=1}^k V_M^{\text{eff}(i)} \right) \Phi_M^{A(k)}. \quad (\text{A.24})$$

Our explicit model calculations so far have been performed in lowest order, *i.e.* with $V_M^{\text{eff}} \simeq V_M^{\text{eff}(1)}$ and $\Phi_M^A \simeq \Phi_M^{A(1)}$ as given by eqs. (8) and (9). In this case we find from eq. (A.16)

$$\mathcal{G}_M^{R,1} \simeq \mathcal{G}_M^{R,1(0)} + \mathcal{G}_M^{R,1(1)} = G_{0M} - i G_{0M} \left(\overline{K}_M^{(2)} + V_R^{(3)} - V_M^{\text{eff}(1)} \right) G_{0M} \quad (\text{A.25})$$

such that the Bethe-Salpeter amplitude $\chi_M \simeq \chi_M^{(1)}$ in the corresponding order of approximation is determined by

$$\chi_M^{(1)} = \left[G_{0M} - i G_{0M} \left(\overline{K}_M^{(2)} + V_R^{(3)} - V_M^{\text{eff}(1)} \right) G_{0M} \right] \times (-i) \left[V_A^{(3)} + V_M^{\text{eff}(1)} \right] \Phi_M^{A(1)}. \quad (\text{A.26})$$

References

1. N. Isgur, G. Karl, Phys. Rev. D **18**, 4187 (1978); **19**, 2653 (1979).
2. S. Godfrey, N. Isgur, Phys. Rev. D **32**, 185 (1985); S. Capstick, N. Isgur, Phys. Rev. D **34**, 2809 (1986).
3. L. Glozman *et al.*, Phys. Rev. C **57**, 3406 (1998); Phys. Rev. D **58**, 094030 (1998).
4. R.F. Wagenbrunn, S. Boffi, W. Klink, W. Plessas, M. Radici, Phys. Lett. B **511**, 33 (2001); L.Ya. Glozman, M. Radici, R.F. Wagenbrunn, S. Boffi, W. Klink, W. Plessas, Phys. Lett. B **516**, 183 (2001).
5. M. Koll, R. Ricken, D. Merten, B. Metsch, H. Petry, Eur. Phys. J. A **9**, 73 (2000).
6. U. Löring, K. Kretzschmar, B.Ch. Metsch, H.R. Petry, Eur. Phys. J. A **10**, 309 (2001).
7. U. Löring, B.Ch. Metsch, H.R. Petry, Eur. Phys. J. A **10**, 395 (2001).
8. U. Löring, B.Ch. Metsch, H.R. Petry, Eur. Phys. J. A **10**, 447 (2001).
9. G. 't Hooft, Phys. Rev. D **14**, 3432 (1976).
10. M.A. Shifman, A.I. Vainshtein, V.I. Zakharov, Nucl. Phys. B **163**, 46 (1980).
11. W.H. Blask, U. Bohn, M.G. Huber, B.C. Metsch, H.R. Petry, Z. Phys. A **337**, 327 (1990).
12. D.I. Diakonov, V.Y. Petrov, Nucl. Phys. B **245**, 259 (1984).
13. K. Kretzschmar, *Electroweak form factors in a covariant quark model of baryons*, PhD Thesis, University of Bonn, TK-01-01.
14. P. Mergell, U.-G. Meißner, D. Drechsel, Nucl. Phys. A **596**, 367 (1996).
15. C. Herberg *et al.*, Eur. Phys. J. A **5**, 131 (1999).
16. M. Ostrick *et al.*, Phys. Rev. Lett. **83**, 276 (1999).
17. I. Passchier *et al.*, Phys. Rev. Lett. **81**, 4988 (1999).
18. T. Eden *et al.*, Phys. Rev. C **50** R1749.
19. R. Schiavilla, I. Sick, Phys. Rev. C **64**, 041002 (2001).
20. H. Anklin *et al.*, Phys. Lett. B **428**, 248 (1998).
21. G. Kubon *et al.*, Phys. Lett. B **524**, 26 (2002).
22. M.K. Jones *et al.*, Phys. Rev. Lett. **84**, 1398 (2000); O. Gayou *et al.*, Phys. Rev. Lett. **88**, 092301 (2002).
23. B.D. Keister, S. Capstick, *N* Physics*, edited by T.-S. H. Lee, W. Roberts (World Scientific, Singapore, 1997) p. 341.
24. E. Tomasi-Gustafsson, M.P. Rekalo, Europhys. Lett. **55**, 188 (2001); nucl-th/0111031.
25. A. del Guerra *et al.*, Nucl. Phys. B **99**, 253 (1985); **107**, 65 (1976).
26. P. Brauel *et al.*, Phys. Lett. B **45**, 389 (1973).
27. E. Amaldi *et al.*, Nuovo Cimento A **65**, 377 (1970); Phys. Lett. B **41**, 216 (1972).
28. P. Joos *et al.*, Phys. Lett. B **62**, 230 (1976).
29. E.D. Bloom *et al.*, Phys. Rev. Lett. **30**, 1186 (1973).
30. Particle Data Group (D.E. Groom *et al.*), Eur. Phys. J. C **15**, 1 (2000).
31. V. Bernard, L. Elouadrhiri, U.-G. Meißner, J. Phys. G **28**, R1 (2002).
32. W. Bartel *et al.*, Phys. Lett. B **28**, 148 (1968).
33. F. Foster, G. Hughes, Rep. Prog. Phys. **46**, 1445 (1983).
34. S. Stein *et al.*, Phys. Rev. D **12**, 1884 (1975).
35. V.V. Frolov *et al.*, Phys. Rev. Lett. **82**, 45 (1999).
36. V. Burkert, Research Program at CEBAF II, edited by V. Burkert *et al.* (CEBAF, USA, 1986) p. 161.
37. C. Gerhardt, Z. Phys. C **4**, 311 (1980).
38. R. Thompson *et al.*, Phys. Rev. Lett. **86**, 1702 (2001).
39. C.S. Armstrong *et al.*, Phys. Rev. D **60**, 052004 (1999).
40. B. Krusche *et al.*, Phys. Rev. Lett. **74**, 3736 (1995).
41. F. Brasse *et al.*, Z. Phys. C **22**, 33 (1984).
42. H. Breuker *et al.*, Phys. Lett. B **74**, 409 (1978).
43. F. Brasse *et al.*, Nucl. Phys. B **139**, 37 (1978).
44. J. Alder *et al.*, Nucl. Phys. B **91**, 386 (1975).
45. U. Beck *et al.*, Phys. Lett. B **51**, 103 (1974).
46. P. Kummer *et al.*, Phys. Rev. Lett. **30**, 873 (1973).
47. T. Sato, T.-S.H. Lee, Phys. Rev. C **63**, 055201 (2001).
48. S.S. Kamalov, Shin Nan Yang, Phys. Rev. Lett. **83**, 4494 (1999).
49. S. Capstick, B.D. Keister, Phys. Rev. D **51**, 3598 (1995).
50. R. Koniuk, N. Isgur, Phys. Rev. D **21**, 1868 (1980).